An Experimental Investigation Replicating the Surface Behavior of Ground Steel Gears in Mixed Lubrication Using Twin-Disk Testing Part 2: Micropitting

W. M. Britton, A. Clarke & H. P. Evans

Published online: 12 Aug 2024.

Submit your article to this journal ✎

Article views: 79

View related articles ✎

View Crossmark data ✎

stle
Society of Tribologists
and Lubrication Engineers

An Experimental Investigation Replicating the Surface Behavior of Ground Steel Gears in Mixed Lubrication Using Twin-Disk Testing Part 2: Micropitting

W. M. Britton[a,b], A. Clarke[b], and H. P. Evans[b]

[a]BMT Limited, Bath, UK; [b]Cardiff University School of Engineering, Cardiff, UK

ABSTRACT

Tooth surfaces in heavily loaded power-transmission gearing can often suffer from surface fatigue on the surface roughness scale, known as micropitting. In this paper, the influence of three variables (pressure, slide-roll ratio, and entrainment velocity) on micropitting is investigated using a full-factorial experimental program using a twin-disk test rig. The results showed that pressure was most influential on micropitting growth during the latter phases of the test, with slide-roll ratio being a more important factor during micropit initiation. The full-factorial nature of these tests allowed two- and three-factor effects to be investigated, demonstrating that micropitting is a complex phenomenon influenced by a network of interconnected effects.

Introduction

Micropitting is a surface fatigue mechanism commonly encountered in heavily loaded gears—perhaps most notably in the slow-moving gears found in wind turbine drive trains. (1, 2) Also known as "grey staining," micropitting can begin mildly. Incipient micropitting is recognizable from the grey or frosted appearance of the surface (3) and may progress to cause catastrophic failure due to stress concentrations as micropits accumulate.

For ground surfaces micropitting occurs along asperity ridges, which carry a disproportionate share of the load and are most aggressively deformed by the running-in process. Micropitting is most prevalent in the dedendum region of gear teeth. (4) Micropitting is also known to be dependent on the direction of sliding, the surface micro-cracks which lead to micropitting growing always in the opposite direction to the sliding/traction, and being inclined at between 10° and 30° to the surface. (5–8) This directionality of micropit crack growth has often been used as a fundamental test of proposed mechanisms for micropitting, and must account for the growth of micro-cracks in one direction only. Proposed theories must also account for the observation that pits do not occur unless a lubricant is present. (9) Such theories include crack-pressurization and fluid entrapment, both cases in which pressurized lubricant drives the growth of cracks. (10) Changes in material properties due to near surface stresses, such as martensitic decay and the creation of plastic deformation regions, may also contribute to the creation and growth of cracks due to stress concentrations at grain boundaries. (8, 11, 12) This is far more commonly encountered in bearings, however, (13) and has not

been universally observed or accepted as a mechanism for gear micropitting. (6, 14, 15)

The influence of surface roughness on micropitting has been widely researched, producing broad agreement that greater surface roughness promotes micropitting, while superfinished or highly polished surfaces may forego micropitting entirely. (3, 16–19) This effect is due to the reduction in size of asperities and other textural changes as the surfaces become smoother. Through similar effects, some antiwear additives such as zinc dialkyl dithio-phosphate (ZDDP) have been widely shown to increase micropitting by preserving roughness features that would otherwise be removed by wear processes. (20–25) Conversely, some coatings such as diamond-like-carbon (DLC) may have the opposite effect, preventing micropitting at the cost of increased wear on uncoated counterfaces. (26–29)

Most research shows increased contact pressure results in increased micropitting; (11, 19, 30) however, this has not been the case in all studies, such as Rabaso et al. (31) who found that changing pressure in the $1.5 - 2.5\,\text{GPa}$ range had no effect on the percentage of surface micropitted or the depth of micropits. Running-in load has also been considered as a separate variable with mixed results. In some cases, the elevated load during running-in polished the surface, (19) while in others micropitting increased, possibly due to greater residual stresses from plastic deformation. (14) An increased running-in load has been suggested, as one of a number of proposed approaches of initiating tests with a limited period of harsh conditions, inducing a limited amount of wear on asperity tips with the aim of better distributing load and reducing cyclic stresses. Another proposed

method of achieving a limited amount of wear on asperity tips is to introduce antiwear additives, such as those discussed previously, into the lubricant after a period of running-in, thereby restraining wear after mild polishing is complete. This method was explored in the work of Benjayati et al. (20)

The effect of sliding can be considered in several ways, and both Li and Kahraman (19) and Oila and Bull (11) found increased slide-roll ratio (SRR) promoted micropitting. Kadiric and Rycerz (7), however, found that for SRRs of 0.05, 0.15, and 0.3, the progression of micropitting on the surface was related to the distance over which the surface had slid and was not impacted by the speed of the sliding or the SRR; although, it should be noted that they determined the extent of micropitting by the depth of material removal, which is not a commonly used approach and may overlap fatigue and wear processes. Several other works, however, have highlighted that a high amount of sliding has potential to promote wear, reducing the number of asperity peaks on which micropitting depends. (23, 31–33)

Finally, entrainment velocity has been considered in only a few works, and increased entrainment is typically seen to reduce the amount of micropitting. (11, 19) Entrainment velocity is known to dominate the formation of the lubricant film, and is most likely to benefit the surfaces through increased film thickness—or perhaps more importantly the specific film thickness Λ, (34) which reflects the relationship between the roughness and film thickness. Research into this effect has found that micropitting typically increases as Λ decreases (35, 36) up to a point at which the previously discussed competition between wear and fatigue processes come into effect. (23, 30)

The first part of this paper contains a detailed analysis of the effects of contact pressure, SRR and entrainment on the running in of ground surfaces during the early phase of endurance tests. In this paper, the individual and interaction effects of the same three variables on early-stage micropitting are investigated experimentally by analyzing the results of the endurance tests to develop greater understanding of how micropitting starts in heavily loaded gear contacts.

Method

A twin-disk micropitting rig was used in this work to replicate an elliptical gear tooth contact. This test rig was described in detail in part one of this work (concerning running-in) and so will only be briefly described here. Two disks of case-carburized EN36 steel were used in each test, each disk being 76.2 mm in diameter with a crown of radius 304.8 mm. This gives an elliptical point contact, with an aspect ratio of approximately 4:1, with the minor axis of the ellipse aligned with the entrainment direction. The contact was lubricated using OEP-80 mineral-based gear oil, supplied to the contact at 80 °C. The circumference of each disk was ground transversely (across the disk width), such that the orientation of roughness to the entrainment direction reflects that found in gears. Drive was supplied to the fast shaft from an electric motor via a speed increasing gear. The fast shaft was geared to the slow shaft, the selected gear ratio imposing the desired SRR, as defined in Eq. [1]. The slow shaft was mounted in a pivoting housing to which load was applied by a hydraulic ram.

$$SRR = \frac{2|u_f - u_s|}{u_f + u_s} \qquad [1]$$

A two-level factorial test program, in which each variable has a "high" setting and a "low" setting, was adopted to allow the maximum information on the effects of Hertzian contact pressure, SRR, and entrainment to be found with the minimum number of tests. One high and one low setting was adopted for each variable, resulting in a total of eight tests. Factorial tests allow the individual effect of each variable to be established by calculating the difference between the average of all tests where the particular variable was at the high setting, and all tests where the particular variable was at the low setting. The effects of interactions between two- and three- variable combinations can also be established in a similar fashion—references to useful resources (37, 38) have been included for readers unfamiliar with this approach. An additional centerpoint test, in which all variables were set halfway between their high and low settings, was also performed. This allows nonlinearity in effects to be detected. The resultant test program is shown in

Table 2. Number of fast disk cycles per test stage.

Test Stage	Fast Disk Cycles This Stage x 10^3	Cumulative Fast Disk Cycles x 10^3
1	3	3
2	3	6
3	14	20
4	30	50
5	50	100
6	100	200
7	100	300
8	100	400
9	200	600
10	400	1000
11	500	1500
12	500	2000

Table 1. Test conditions.

Test	Max Pressure/GPa	SRR	Entrainment Velocity/ms^{-1}	Fast Disk Ra/μm	Slow Disk Ra/μm	Specific Film Thickness, Λ
Test 1	1.6	0.500	4.0	0.42	0.43	0.23
Test 2	1.6	0.500	2.0	0.39	0.40	0.19
Test 3	1.6	0.250	2.0	0.37	0.44	0.24
Test 4	1.2	0.500	2.0	0.41	0.41	0.27
Test 5	1.2	0.250	4.0	0.41	0.38	0.44
Centerpoint	1.4	0.375	3.0	0.46	0.41	0.27
Test 6	1.6	0.250	4.0	0.45	0.46	0.29
Test 7	1.2	0.250	2.0	0.45	0.46	0.26
Test 8	1.2	0.500	4.0	0.43	0.46	0.35

Abbreviation: SRR, slide-roll ratio.

Table 1, including specific film thickness for each test determined using the surface Rq values at the conclusion of running-in.
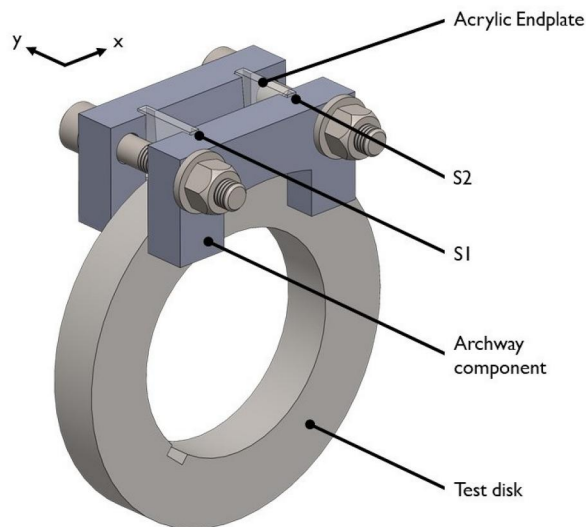

Figure 1. Arch arrangement clamped to a disk for replica casting.

The tests comprised an initial running-in process of 6,000 fast disk cycles across two test stages, followed by 10 further test stages reaching a total of 2 million fast disk cycles. The test stages are detailed in Table 2.

Between each test stage, replicas of the surface were made using Acrulite® Microtech Type A, a PMMA-based replica material. The surface was prepared by spray application of a chemical degreaser, followed by careful wiping clean. A pair of steel archways were clamped to each disk, as can be seen in Fig. 1, and acrylic endplates were inserted into slots S1 and S2 at each end to provide a well for the replication liquid. The areas behind the endplates and below the archways were then packed with plasticine to prevent leakage. The replication liquid was then poured into the replication area and allowed to cure for 1 h. The archways were then removed and the replica detached from the surface. The replicas were then checked for defects under an optical microscope and the replication process repeated if any defects were observed.

Successful replicas taken after test stages 2, 4, 5, 6, 8, 10, and 12 were scanned using a Taylor Hobson Form Talysurf Series 2 surface profilometer with automatic y-stage, as were the true disk surfaces before and after testing. Each areal scan was 6 mm long in the circumferential (x) direction and
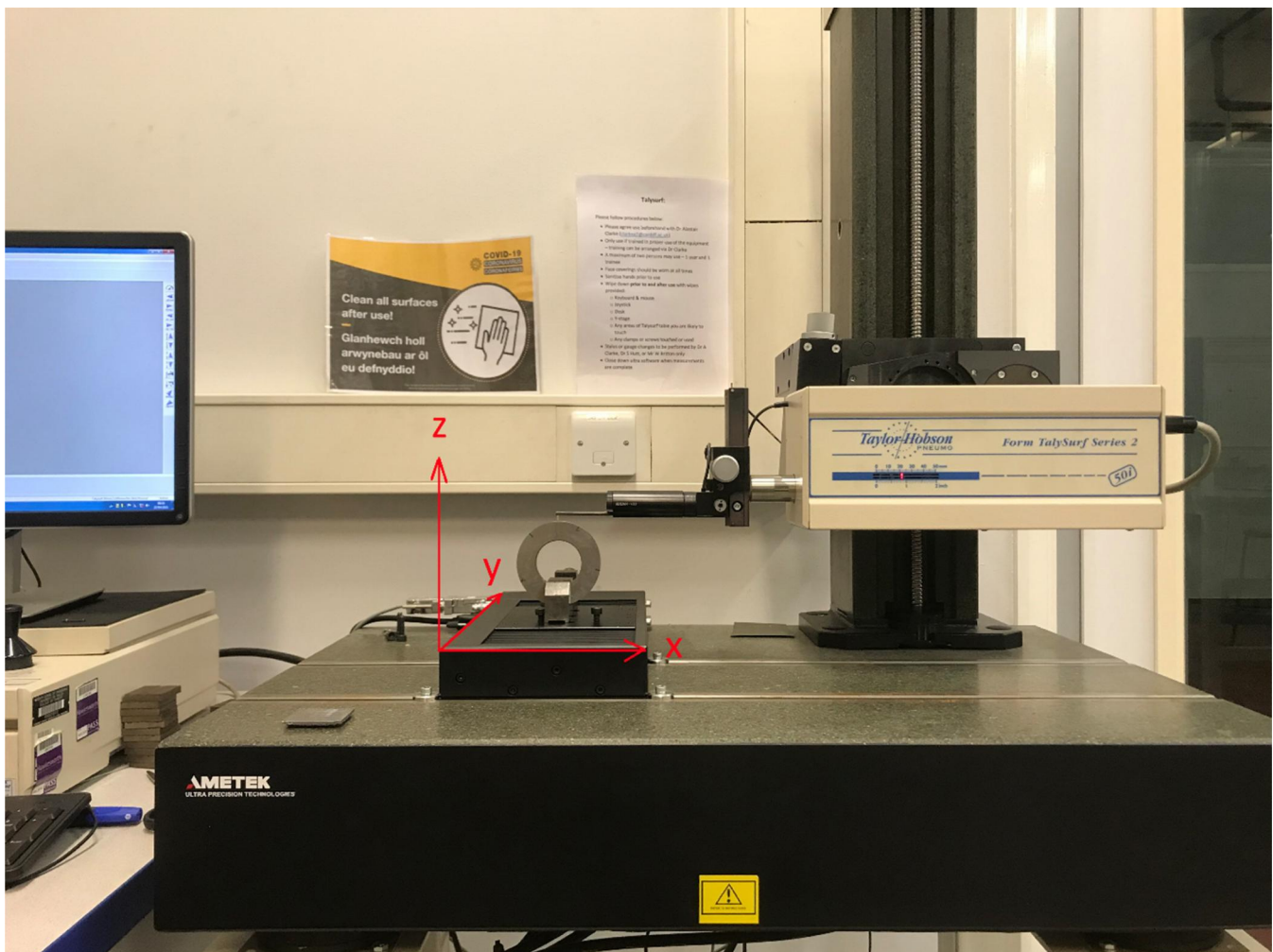

Figure 2. A disk being scanned on the surface profilometer.

typically 7 mm in the axial y-direction. A data point spacing (dx) of 0.5 µm was adopted in the x-direction, with a spacing of 3 µm (dy) between profiles in the y-direction. This mis-match in resolution reflects the fact that the surface roughness lay is nominally aligned to the y direction. Figure 2 shows the arrangement for areal scanning of a disk.

A micropit detection algorithm was applied to identify micropits in the ground surface by the localized gradients, based upon the observation that micropit edges are typically the steepest features on the surface. This algorithm was developed and explained in detail in previous work. (39) As was detailed in that work, an adjustment factor of 0.723 was applied to correct the detected percentage of surface micropitted determined on Acrulite replicas. The true disk surface (after removal from the rig) was used to obtain end-of-test values. Figure 3 shows a scan of a micropitted disk,

including the hardness marks used to help in relocation, alongside a close up of a micropitted section.

In addition to the percentage of the surface micropitted, the rate of micropitting, depth of the deepest 5% of micropitted points, cycles to reach 3% micropitted, and the total volume removed by micropitting per unit area at the end of testing were also estimated. As heights of points in a gaussian filtered surface are given relative to the mean height of the surface, and micropits are known to form from previous asperities (which sit above the mean line), a volume simply calculated from the mean line of the surface is an inappropriate measure. Instead, the mean height of all non-micropitted points along an asperity was calculated—making the assumption that asperities are essentially extruded surfaces which are largely constant (or only gradually changing) across their length. It was then assumed that any
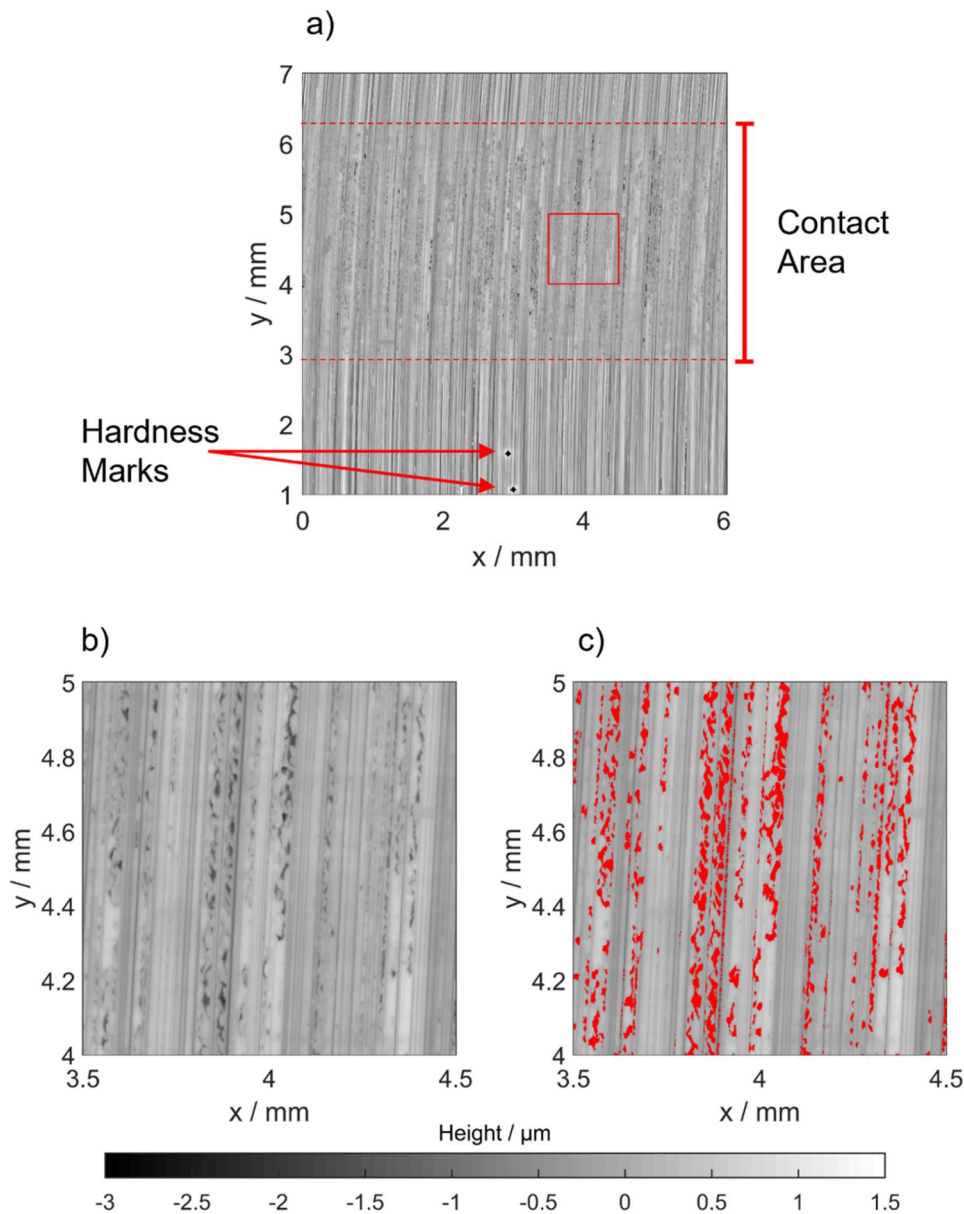

Figure 3. a) A Surface scan with the hardness marks indicated. The area indicated by the red square is shown more closely in b) and detected micropits are overlaid in red in c).

micropitted points along that asperity were initially at this height, and the volume removed at each micropitted point was calculated as the height change relative to this new datum height × dx × dy.

Results

As was discussed in the first part of this work, Tests 1 and 2 exhibited wear behavior during the running-in process. Test 1 took the form of a single continuous band approximately 2 mm wide through the center of the contact area, while for Test 2 isolated islands of wear were observed. As micropitting began to occur, it became clear that these regions of wear possessed a resistance to micropitting, and this persisted throughout the tests as can be seen in Fig. 4. This was the case for both fast and slow surfaces in each test.

As this work was attempting to discern the effects of pressure, SRR, and entrainment on micropitting without the effect of wear, the wear-affected areas on these surfaces were excluded from analysis. The area for exclusion was manually defined on the surface at the end of test and then relocated to match in all of the earlier surfaces. They are indicated by the regions bounded by red dashed lines on Fig. 4.

Percentage of surface micropitted at end of test

This parameter considers the percentage of the contact area micropitted after 2 million Fast Disk cycles. The points in each graph represent the average value for all tests where the particular parameter was high, and all tests where the particular parameter was low. For example, for the fast
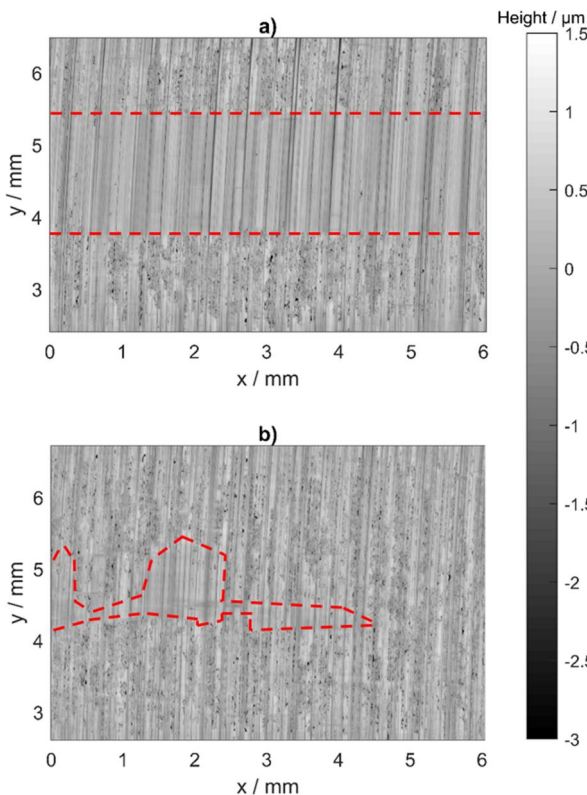
surface pressure effect, the point at 1.2 GPa represents the average result of all tests with a 1.2 GPa maximum pressure (regardless of the settings of entrainment velocity and SRR for these tests), and the same for the point at 1.6 GPa (again regardless of the settings of the other parameters). The difference between the two points indicates the effect of pressure on the output. This is the same method as followed for running-in in the first part of this paper. As shown in Fig. 5, the pressure caused the largest increase in micropitted area on both fast and slow surfaces. SRR exhibited a similar effect on the fast surface, however had negligible influence on the slow surface. A similar disagreement between the fast and slow surface effects was seen for entrainment, which showed a moderate protective effect on the fast surface, where increased entrainment reduced the amount of micropitting, but showed no strong influence on the slow surface. The centerpoint test results, indicated by a
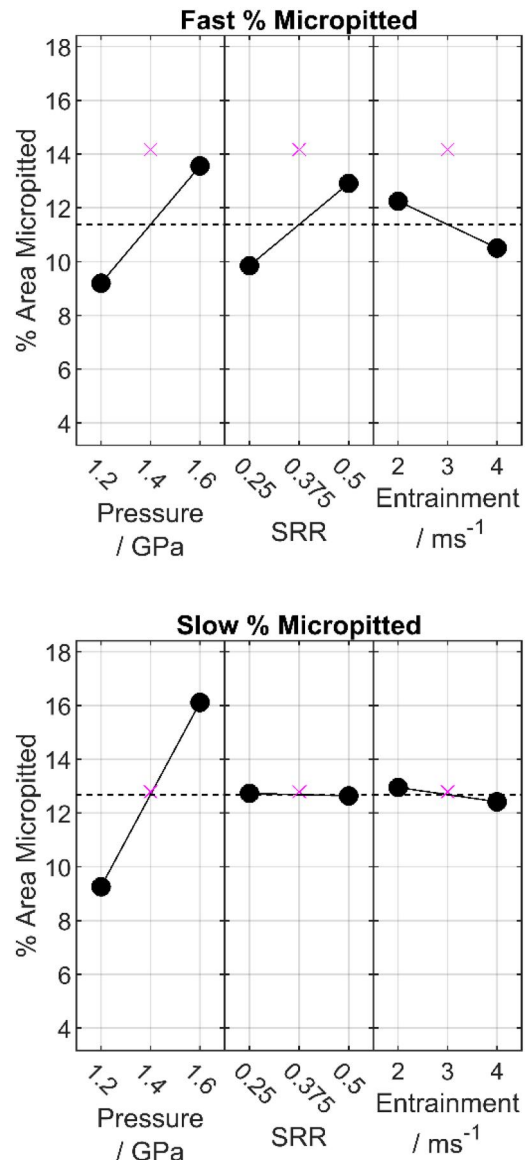

Figure 4. Fast surfaces of a) test 1 and b) test 2 at the end of test.

Figure 5. Main effects of pressure, slide-roll ratio (SRR), and entrainment on percentage of surface micropitted after 2 million fast disk cycles. In each case, the cross indicates the result of the centerpoint test while the dashed line indicates the mean value for all tests.

cross, sat on the lines for the slow surface, indicating linear behavior; however, the centerpoint was located away from the lines on the fast surface, showing nonlinear effects to be present.

Two-factor interaction plots for the percentage of surface micropitted at end of test can be seen in Fig. 6. In each plot, one parameter is changed on the x-axis, while the high or low setting of the other parameter is represented by solid or dashed lines respectively. For example, the fast surface plots in Fig. 6 marked a) illustrate the interaction between pressure and SRR, b) pressure and entrainment velocity, and c) entrainment velocity and SRR. Where lines remain parallel, this indicates that there is no interaction between the two variables. Where the angle of the line changes between the high and low settings, an interaction effect is present. The stronger the two-factor interaction effect, the more pronounced the change in angle.

Strong interactions between pressure and SRR were observed for both fast and slow surfaces. For both surfaces increases in pressure were seen to produce a greater increase in micropitting when SRR was low. SRR had a stronger increasing effect on micropitting at low pressure for the fast surface. However, on the slow surface, the direction of the
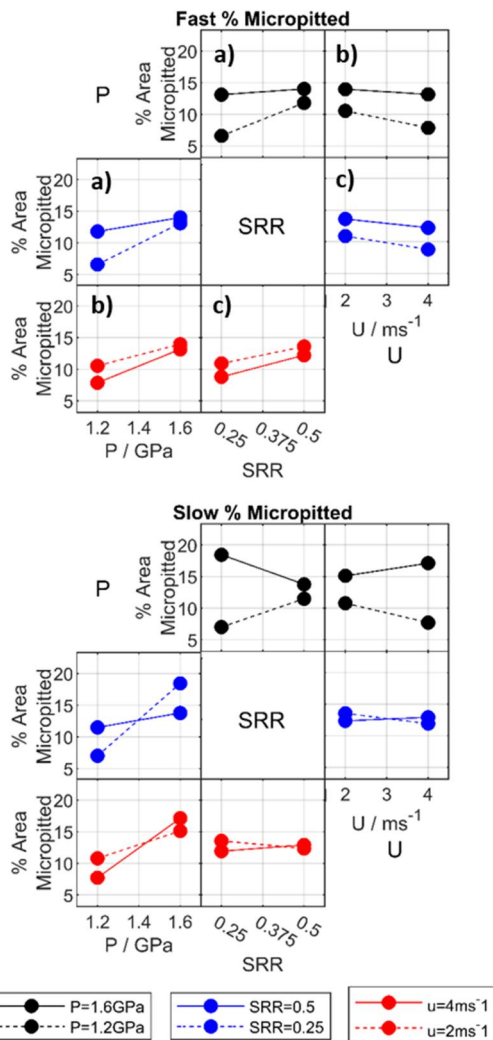
SRR effect was seen to change with pressure with increases in SRR at high pressure that lowered the percentage micropitted.

Where two-factor interactions are affected by changes in a third variable, this indicates the presence of a three-factor interaction. In the three-factor interaction plots such as those shown in Fig. 7, if the two factor effect between two variables (i.e., the angle between the lines) changes when a third variable is changed, the presence of a three-factor effect is indicated. For example, Fig. 7a shows the interaction between pressure and SRR when entrainment is low, and the lines are parallel indicating no two-factor effect. In
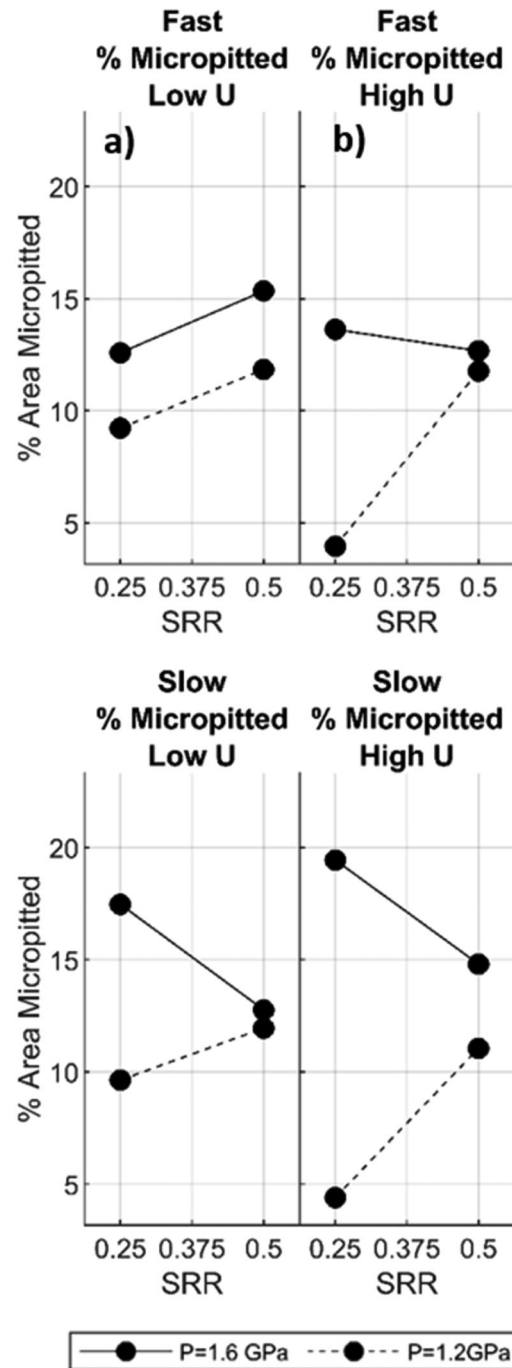

Figure 6. Two-factor interaction plots for percentage of surface micropitted after 2 million fast disk cycles.

Figure 7. Change in the pressure- slide-roll ratio (SRR) two-factor interaction for % micropitted after 2 million fast disk cycles with entrainment.
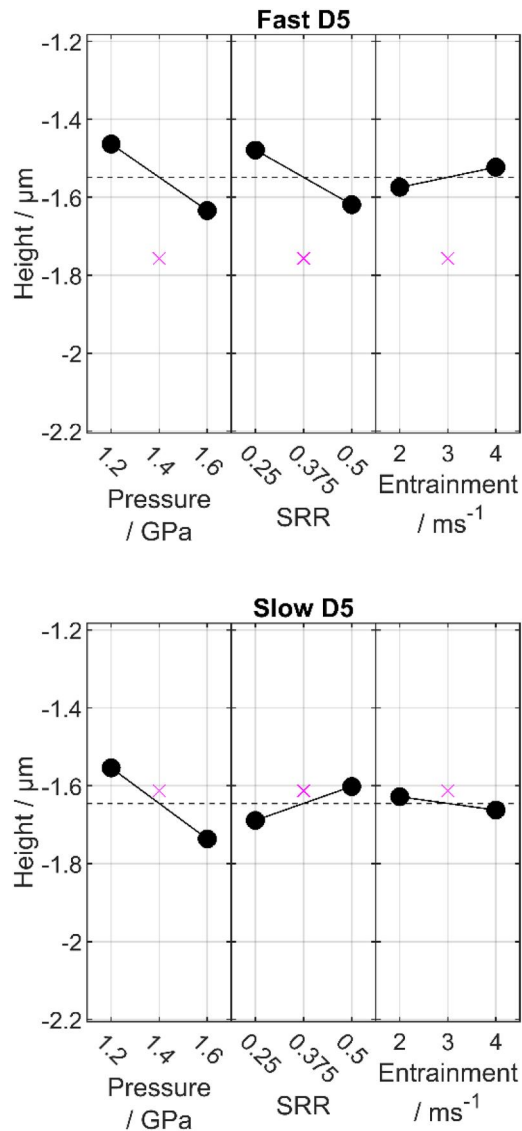
Figure 8. Main effects of pressure, slide-roll ratio (SRR) and entrainment on mean height of deepest 5% of micropitted points.

Figure 9. Two factor interaction plots for height of deepest 5% of micropitted points.

Fig. 7b, where entrainment is high, a two factor effect is present—this change indicates a three factor effect is present. The angle of incidence of the two lines for the pressure-SRR interaction changed for both the fast and slow surfaces, showing a three factor effect was present for the percentage of surface micropitted after 2 million fast disk cycles on both surfaces.

Deepest micropitted points

The points that reside in a micropit may be at a large range of depths, the rim of the micropit often residing above the mean line of the surface (because micropits occur on asperities) and points then being measured descending steep slanted sides. As such, a mean depth of all micropitted points relative to the mean line does not provide an adequate reflection of depth of the bottom of the micropits. H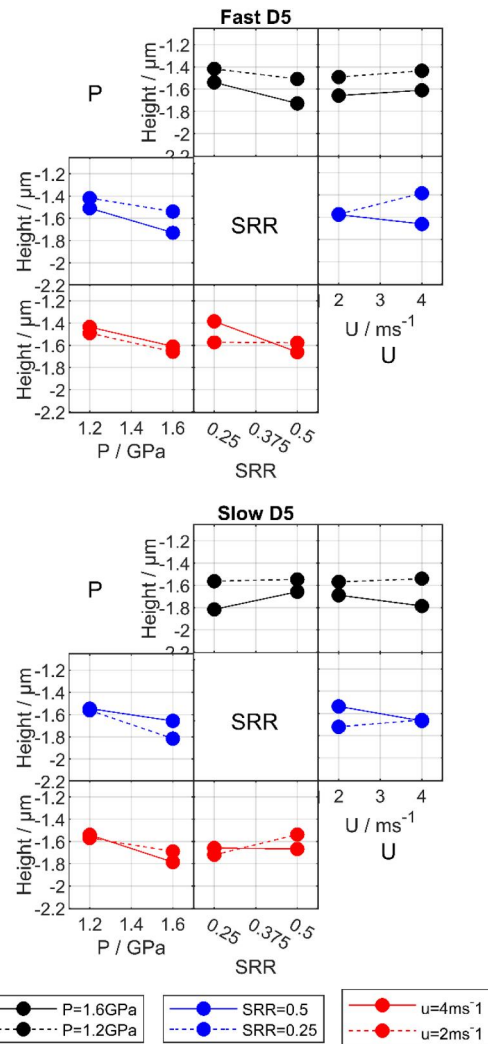owever, by taking the average height of the deepest 5% of micropitted points, henceforth referred to as D5, it is hoped to achieve a more representative value for micropit depth. This value was taken from the measured disk surface at the end of test.

The main effects for D5 are shown in Fig. 8. For both fast and slow surfaces, pressure had a significant effect, deepening micropits by 0.17 μm and 0.18 μm, respectively. On the fast surface, SRR also decreased the average height by only 0.03 μm less than pressure; however, the effect of SRR on the slow surface was in the opposite direction, leading to shallower micropits. Closer inspection showed a clear offset between values at high and low SRR for the fast surface, while the groups overlapped significantly on the slow. It is likely, therefore, that the slow surface SRR effect is smaller than calculated, but requires further experimentation to confirm. For entrainment, there was further disagreement between fast and slow surfaces, entrainment showing a small protective effect on the fast surface, but a smaller magnitude detrimental effect on the slow surface. Again, the overlap in slow surface results suggest the slow surface effect to be smaller than shown.
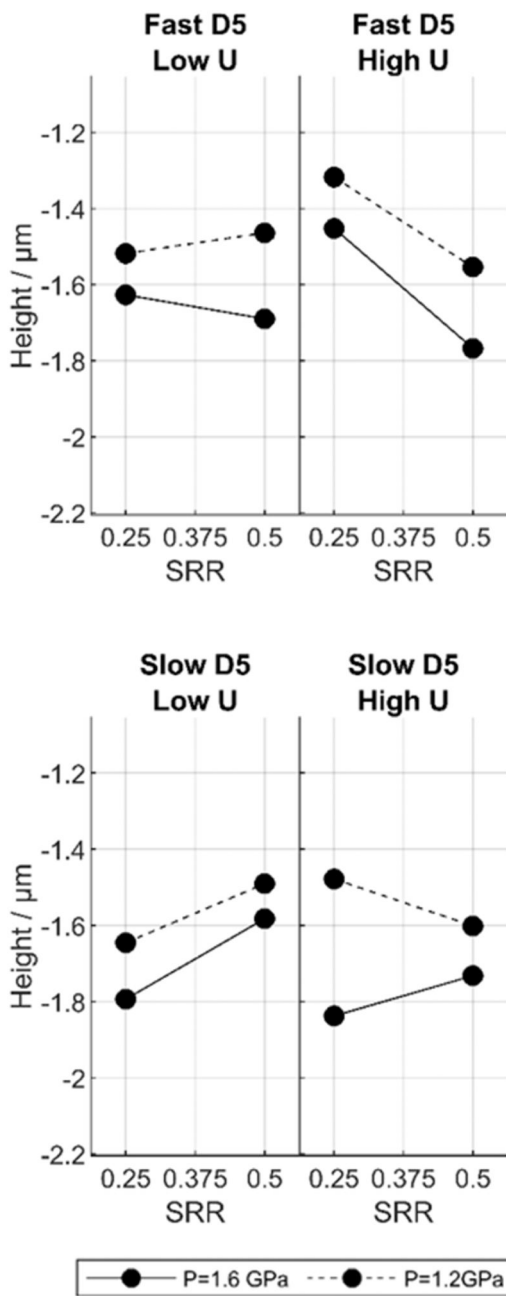
Figure 10. Change in pressure- slide-roll ratio (SRR) two-factor interaction for height of deepest 5% of micropitted points with entrainment.

The centerpoint test result suggested significant nonlinearity in the fast surface results, but was only very slightly removed from the line for the slow surface results.

The two-factor interaction plots for D5 are shown in Fig. 9. Only a weak pressure-SRR interaction was observed on the fast surface. In both cases, increases in pressure or SRR having a mildly stronger influence when the other variable was set high. The slow surface interaction was stronger and acted in the opposite sense to that on the fast surface. No interaction between pressure and entrainment was observed on the fast surface, while increases in both pressure and entrainment were observed to have a greater height-reducing effect when the other variable was set high. SRR and entrainment interacted strongly on both surfaces, but in opposite senses.
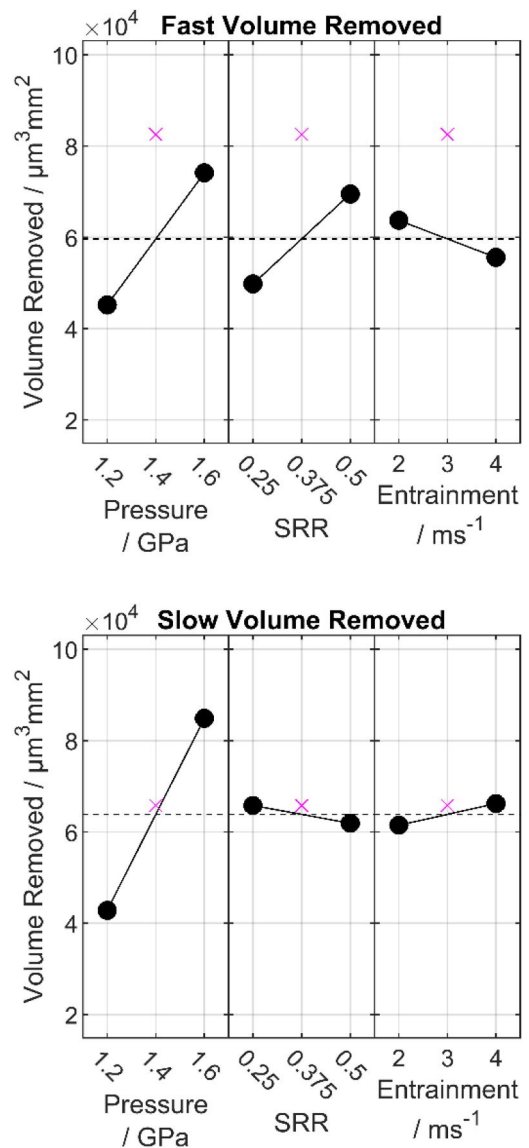

Figure 11. Main effects of pressure, slide-roll ratio (SRR), and entrainment on the volume of material removed.

Figure 10 shows a minimal change in the included angle between the two lines at high and low entrainment for the fast surface—indicating no three-factor effect present. For the slow surface, however, there is a difference between the pressure-SRR interaction at low and high entrainment; hence, a three-factor interaction was present for the slow surface.

Volume removed

The volume of material removed through micropitting per unit area was evaluated from the end of test disk surface using the methods discussed previously. The main effects on volume removed (Fig. 11) were similar to those seen previously for percentage of area micropitted at the end of the test, suggesting micropitted area and volume are strongly related. Pressure was again seen to have the largest effect on both surfaces, with an increase in pressure increasing the
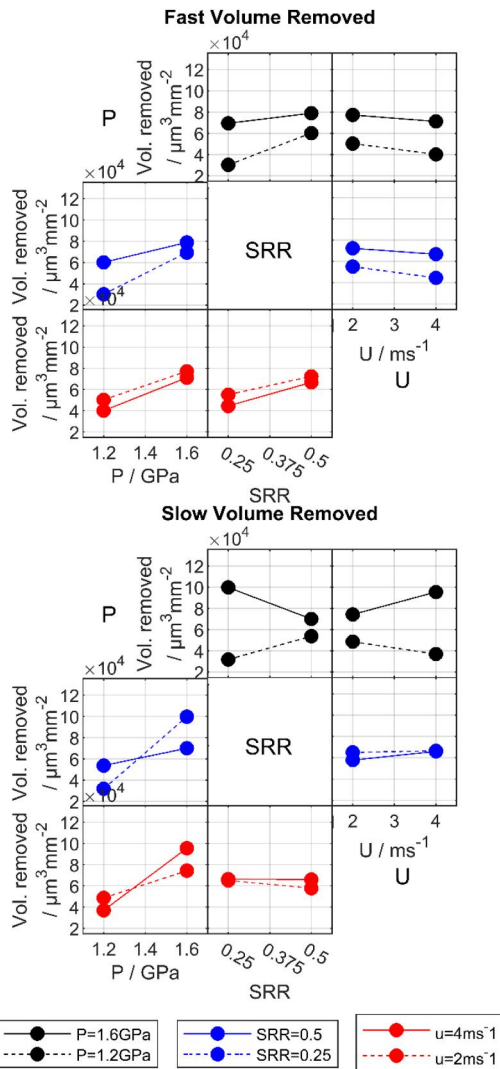
Figure 12. Two factor interaction plots for the volume removed per unit area.

volume removed. On the fast surface, SRR was the second strongest effect, also increasing the volume removed as SRR increased, while a weaker entrainment effect served to protect the surface, with volume removed reducing at higher entrainment. On the slow surface, SRR and entrainment both showed only weak effects in the opposite sense to that seen on the fast surface: increases in SRR caused a slight decrease in volume removed, while increased entrainment caused a slight increase in volume removed.

Again, the fast surface centerpoint test result was significantly removed from the lines, indicating highly nonlinear effects. For the slow surface, the centerpoint was very close to the line, indicating a near-linear effect.

The two-factor interaction effects on volume removed are shown in Fig. 12. Two-factor interactions were present between pressure and SRR on both surfaces, but differed in nature, as they did for the percentage of surface micropitted. On the fast surface, pressure-entrainment and SRR-entrainment interactions were not observed, the lines in both cases being parallel or near-parallel. On the slow surface, however, pressure increased volume removed more greatly when the entrainment was high, while entrainment influenced volume removed in different directions depending on the pressure.
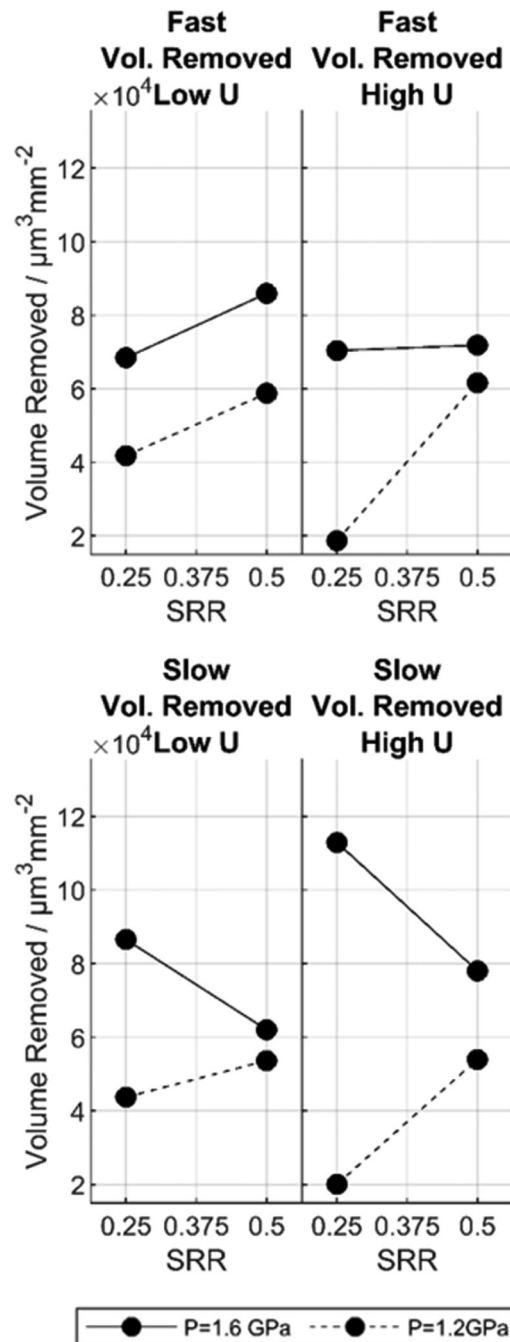

Figure 13. Change in pressure- slide-roll ratio (SRR) two-factor interaction for volume removed per unit area with entrainment.

Only the combination of high sliding and low speed influenced the outcome for the entrainment-SRR interaction.

As can be seen in Fig. 13, three factor interactions were present on both surfaces for the volume removed parameter.

Cycles to reach 3% micropitted

The highest integer of percentage micropitted reached by both fast and slow surfaces in all tests was 3%; hence, the approximate number of fast disk cycles to reach this milestone was recorded for each test. This was calculated assuming a linear progression of micropitting between areal
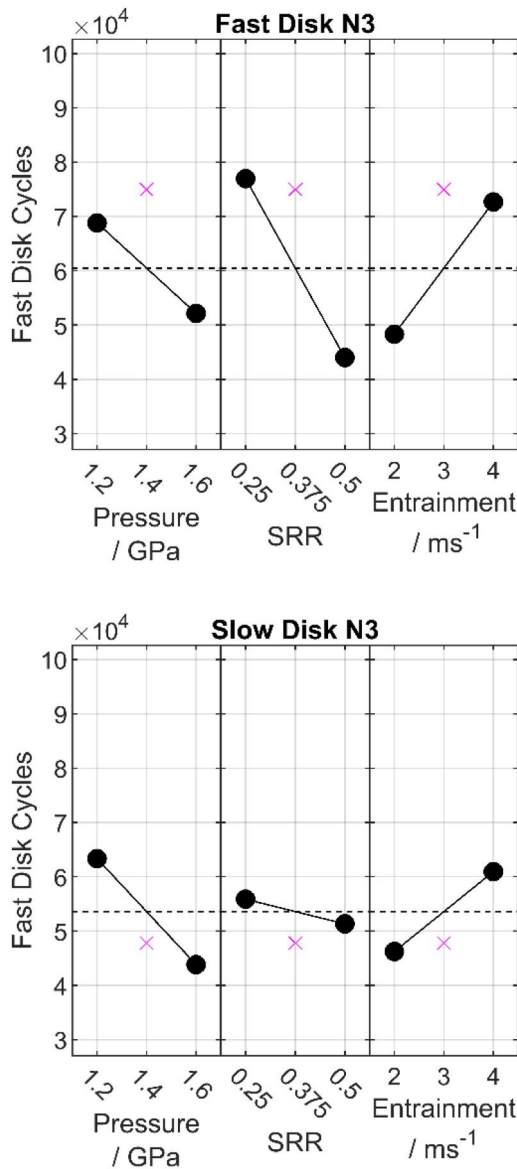
Figure 14. Main effects of pressure, slide-roll ratio (SRR), and entrainment on the number of fast disk cycles to reach 3% micropitted.

Figure 15. Two factor interaction plots for the number of fast disk cycles to reach 3% micropitted.

surface measurement data points. Figure 14 shows the main effect influences on this parameter, henceforth referred to as N3.

SRR had the strongest influence on the fast surface, higher SRR reducing the number of cycles to reach 3% micropitted. In contrast, this was the smallest effect on the slow surface. Pressure had a similar magnitude effect to reduce N3 on both surfaces, while entrainment showed a strong N3-increasing influence on both surfaces. In all cases, the centerpoint was distanced from the main effect lines indicating nonlinearity in the response.

The two-factor interaction plots for N3 are shown in Fig. 15. Pressure and SRR interacted on both surfaces—in both cases the effect of pressure being stronger when SRR was set low, and vice versa. As indicated by the parallel lines, pressure and entrainment did not interact on the fast surface; however, for the slow surface the sole condition of low pressure and high entrainment significantly increased
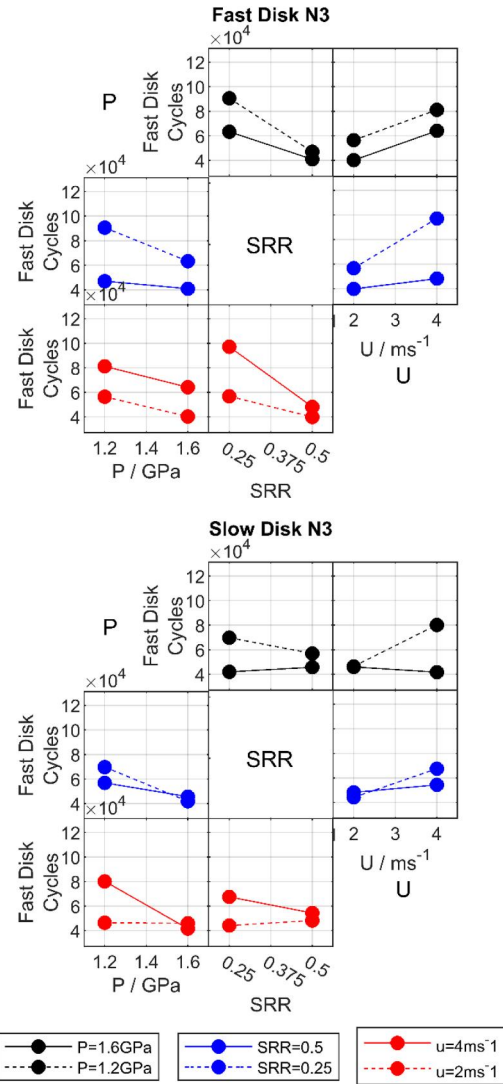
N3. On both surfaces, SRR had a stronger effect alongside high entrainment, while entrainment had a stronger influence at low SRR.

As can be seen in Fig. 16, for both fast and slow surfaces, the interaction between pressure and SRR was of lower magnitude when entrainment was set high. This indicates the presence of a three-factor interaction effect, most strongly seen on the slow surface.

Micropitting rate during test stages 9 and 10

The micropitting rate during test stages 9 and 10 (from $4 \times 10^5 – 1 \times 10^6$ fast disk cycles) was chosen to assess the effects on micropitting rate later in the test as it avoided any effects induced from the change from replica to true disk measurement at the end of test. The rate was calculated per-cycle of the corresponding disk (i.e., per fast disk cycle for the fast surface and per slow disk cycle for the slow surface) assuming a constant rate of micropitting between the surface measurements.
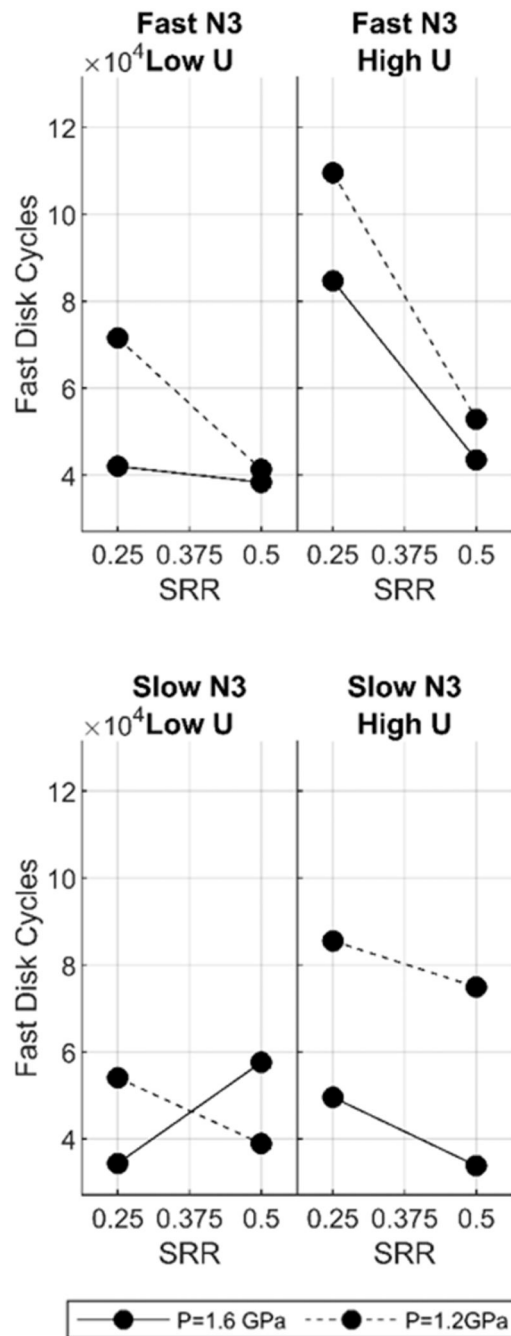
Figure 16. Change in pressure- slide-roll ratio (SRR) two-factor interaction for fast disk cycles to reach 3% micropitted.

Figure 17. Main effects of pressure, slide-roll ratio (SRR), and entrainment on the rate of micropitting during test stages 9 and 10.

The main effects on this late-stage micropitting rate are shown in Fig. 17. For both fast and slow surfaces, increased pressure raised the rate of micropitting and is the dominant variable in late-stage micropitting. On the fast surface, increased SRR also caused a small increase in micropitting rate, while increased entrainment again had a small protective influence on the surface. Both SRR and entrainment had negligible effect on the slow surface. In all cases, the center-point test result does not lie on the mid-point of the line, indicating some degree of nonlinearity.

The two-factor interaction effects on the test stage 9 and 10 micropitting rate are shown in Fig. 18. Interaction effects matched closely 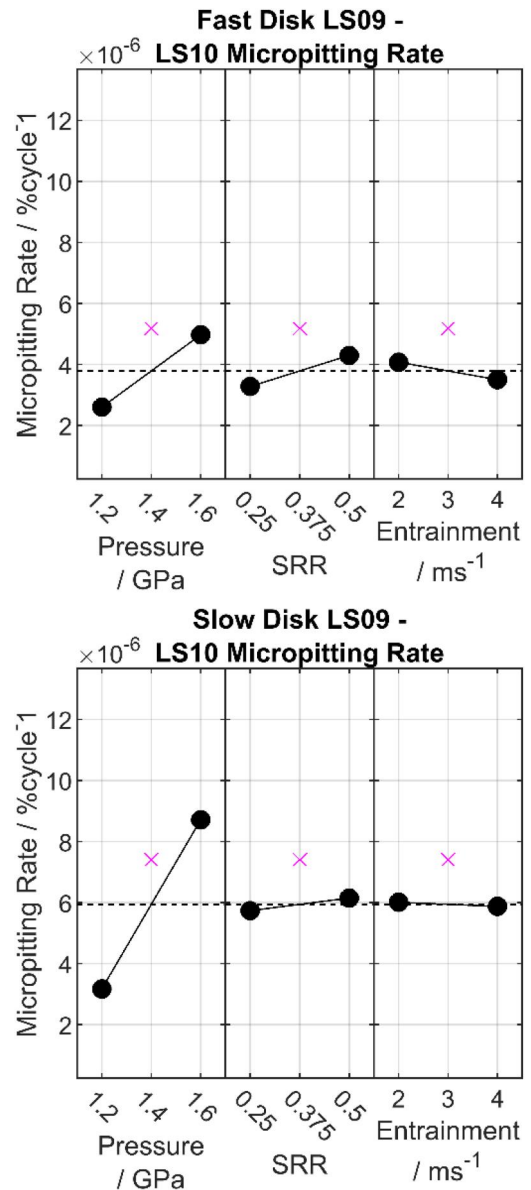on both surfaces, with two-factor interactions observed between all three variables. For both surfaces, the effect of pressure was stronger at low SRR and at high entrainment. The directions of influence of both SRR and entrainment changed depending on whether pressure was high or low, as well as interacting themselves.

As might be expected considering the number of two-factor effects present, three-factor interactions were present for both fast and slow surfaces. This can be seen in Fig. 19.

Early-Stage micropitting

Due to issues with the surface replication, two surface replicas had to be discarded: one from the fast disk at test stage 4 of Test 8, and the other from the slow surface at test stage 5 of Test 2. As a result, different parameters were needed to assess the early stage micropitting of the surface for fast and slow disks.
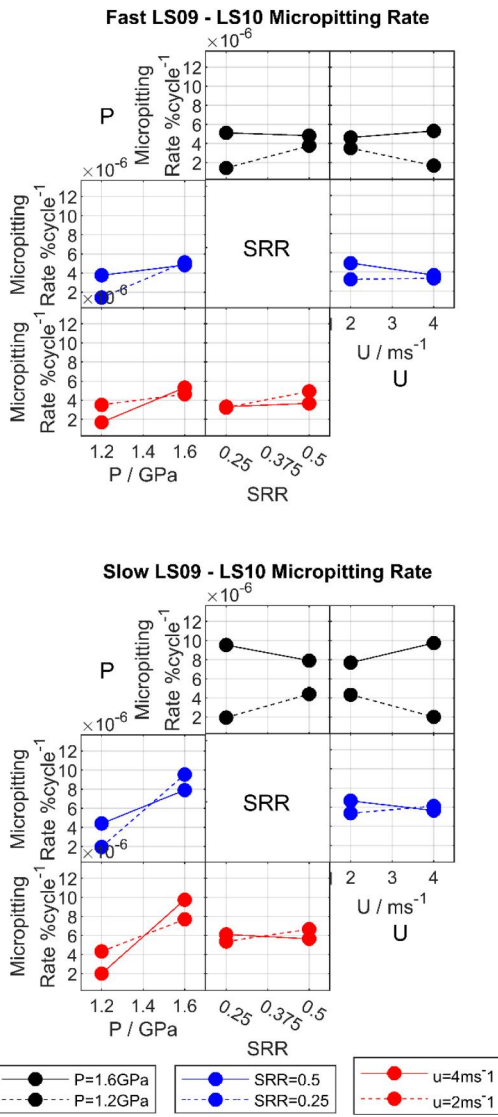
Figure 18. Two factor interaction plots for micropitting rate during test stages 9 and 10.

For the slow surface the peak rate of micropitting, which occurred between test stages 2 and 4, was used. This was not appropriate for the fast surface due to the missing test stage 4 replica. For the fast surface, the percentage of surface micropitted after the next test stage (1×10^5 fast disk cycles) was used. Although different assessments of early-stage micropitting have been used, it is thought that they ought to provide similar indications of the influence of the three test parameters.

As can be seen in Fig. 20, although the parameters themselves were different, the influence of each factor was similar in effect across both surfaces. In both cases, SRR had the strongest influence of the three variables, increasing early-stage micropitting behavior. Increasing pressure also increased micropitting and was the second strongest factor on the slow surface but the weakest on the fast surface. Increased entrainment opposed micropitting in both cases. Again, the centerpoint test result suggested nonlinearity on the fast surface, but linear behavior on the slow.

Two-factor interaction effects for early stage micropitting are shown in Fig. 21. As is clear from this figure, no notable
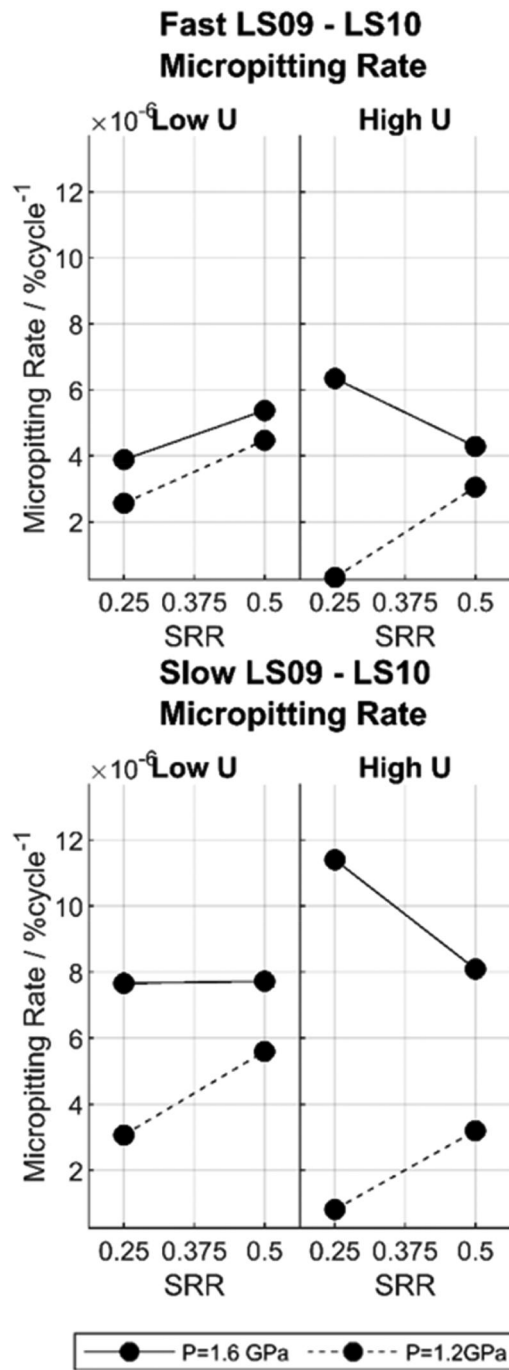
Figure 19. Change in pressure- slide-roll ratio (SRR) two-factor interaction micropitting rate during test stages 9 and 10.

two-factor interactions were present on the fast surface, whereas on the slow surface all three two-factor interactions were present (although the pressure-SRR interaction was small).

Figure 22 shows the three-factor interactions for the early stage micropitting behavior. A weak three-factor interaction can be seen for the fast surface; however, when the distinct lack of two-factor interactions is considered alongside this weak apparent effect, there is a reasonable likelihood that this is perhaps the result of natural variation in outputs. However, further tests would be required to confirm this.

Figure 20. Main effects of pressure, slide-roll ratio (SRR), and entrainment on early-stage micropitting parameters.

Figure 21. Two-factor interaction plots for early-stage micropitting behavior.

A very strong interaction effect is, however, shown for the slow surface.

Table 3 shows the strengths of each main factor and interaction effect on the parameters considered. For single factors, the effect shown is the result of the change from the low to high setting. For interaction effects (variable 1 x variable 2) the tests that constitute a "high" or "low" interaction setting can be established by expressing individual variables (e.g., pressure) set high as 1, and set low as −1. If the product of the variables in an interaction is −1 (e.g., pressure and SRR, or PxSRR) for a given test then that test is at the low setting, and, conversely, if it is 1 then that test is at the high setting. In effect, that means that for two-factor interactions, tests where one variable is high and the other is low are the "low" setting, while tests where both variables are both high or low together are "high." The same logic can be extended to three-factor interactions. As with single variable

effects, the difference between the average values at high and low settings provides the effect of the interaction.

The effects determined in Table 3 may be used to create models of the effects of each variable and their interactions on each output. In this model, P, S, and U represent the settings of pressure, slide-roll ratio, and entrainment velocity, respectively, applied in terms of their coded form (i.e., a pressure value of 1.2 GPa would be −1, and a pressure value of 1.6 GPa would be +1; hence, a pressure of 1.5 GPa would be +0.5). The effects shown in Table 3 divided by two become the coefficients as can be seen in Eq. [2]: the halving of the effects reflecting the fact that each effect is the change across two increments of the scale, as opposed to between 0 and 1.

$$output = \mu + \frac{\beta_1}{2}P + \frac{\beta_2}{2}S + \frac{\beta_3}{2}U + \frac{\beta_{12}}{2}PS + \frac{\beta_{13}}{2}PU + \frac{\beta_{23}}{2}SU$$
$$+ \frac{\beta_{123}}{2}PSU$$

[2]

Fast % Micropitted After 1×10^5 Cycles

Slow Peak Micropitting Rate

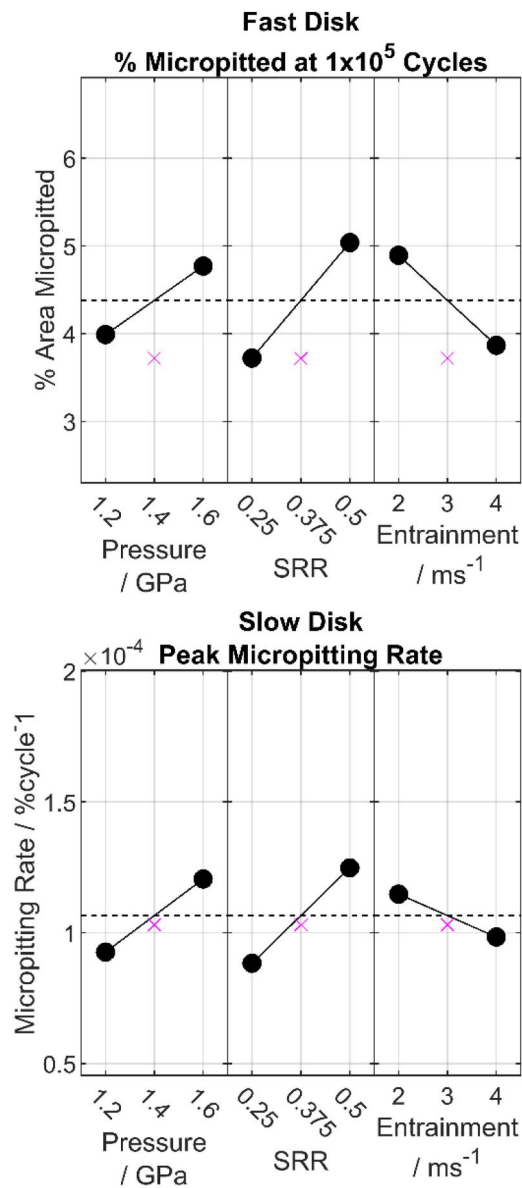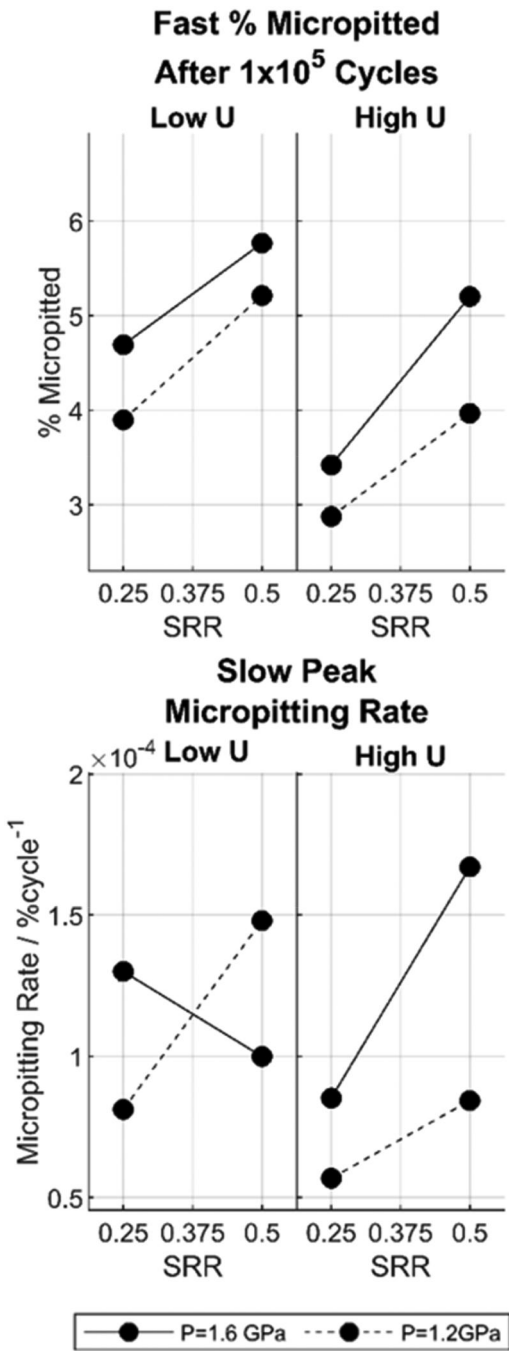**Figure 22.** Change in pressure- slide-roll ratio (SRR) two-factor interaction with entrainment for early stage micropitting parameters.

Discussion

The strong resistance to micropitting observed within areas of mild wear in Tests 1 and 2 was a particularly interesting outcome of this test program. Previous research that has computationally limited the allowed wear in combined wear-fatigue simulations to assess its influence on predicted micropitting (23) has been able to show this effect in theory; however, there is limited experimental work in the literature to show this in real-world tests. In the tests shown here, the occurrences of wear and micropitting were within the same contact, and it is clear that where wear was provoked micro-pitting was severely retarded.

In both of these tests, the highly defined boundary between micropitted and worn areas was particularly notice-able. This suggests the presence of a hard threshold condi-tion at some point in the system, such as surface modification due to wear beyond which micropitting cannot take place. It cannot be known at this point exactly what this threshold is or how it influences the system.

Throughout the experimental program, increased contact pressure showed strong micropitting-increasing effects on both fast and slow surfaces and was the strongest main effect on the percentage of surface micropitted at the end of test, the volume removed through micropitting, micropit depth, and late-stage micropitting rate. While contact pres-sure was also seen to increase micropitting in the earlier stages of the test, reflected in the early-stage micropitting parameters and the N3 parameter, it was not the dominant parameter during early-stage micropitting.

The effect of pressure on the D5 parameter was of similar magnitude for both fast and slow surfaces, which can be rationalized by considering the increase in the depth of maximum shear stress beneath asperity contacts as the pres-sure increases, which is not influenced by differences between the surfaces such as their relative speed. For many other parameters the slow surface pressure effect was larger than that seen for the fast surface; however, the cause of this is unknown.

The magnitudes of the effects of SRR and entrainment differed significantly between the fast and slow surfaces. These differences tended to manifest themselves later in the test however. The early-stage micropitting parameters of peak micropitting rate (slow surface) and percentage

Table 3. Summary of main and interaction effects.

| Parameter (Eq. [2])	Mean output (μ)	P (β_1)	SRR (β_2)	U (β_3)	PxSRR (β_{12})	PxU (β_{13})	SRRxU (β_{23})	PxSRRxU (β_{123})
Fast surface % micropitted/Δ%	11.38	4.36	3.06	−1.74	−2.16	0.93	0.37	2.23
Slow surface % micropitted/Δ%	12.68	6.85	−0.09	−0.53	−4.57	2.53	1.10	1.07
Fast surface D5/$\Delta\mu m$	−1.549	−0.171	−0.140	0.052	−0.049	−0.003	−0.136	−0.010
Slow surface D5/$\Delta\mu m$	−1.645	−0.183	0.087	−0.034	0.071	−0.063	−0.096	−0.043
Fast surface volume removed/$\Delta\mu m^3 mm^{-2}$	59651	28951	19721	−8115	−10243	2051	2491	10505
Slow surface volume removed/$\Delta\mu m^3 mm^{-2}$	63832	42034	−3891	4756	−25800	16428	3398	8605
Fast surface N3/Δ fast disk cycles	60488	−16676	−32952	24329	10521	−413	−15987	2767
Slow surface N3/Δ fast disk cycles	53589	−19521	−4547	14726	8300	−19017	−8617	10869
Fast surface test stage 9 & 10 Micropitting rate/$\Delta 10^{-6}$%cycle^{-1}	3.79	2.37	1.02	−0.58	−1.30	1.26	−0.68	1.10
Slow surface test stage 9 & 10 Micropitting rate/$\Delta 10^{-6}$%cycle^{-1}	5.95	5.55	0.42	−0.14	−2.04	2.19	−0.88	0.81
Fast surface % micropitted at 1×10^5 fast disk cycles/Δ%	4.38	0.78	1.32	−1.03	0.11	0.11	0.12	−0.23
Slow surface peak micropitting rate/$\Delta 10^{-6}$%cycle^{-1}	106.55	27.95	36.50	−16.46	−10.64	27.60	18.15	−37.80

Abbreviation: SSR, slide-roll ratio.
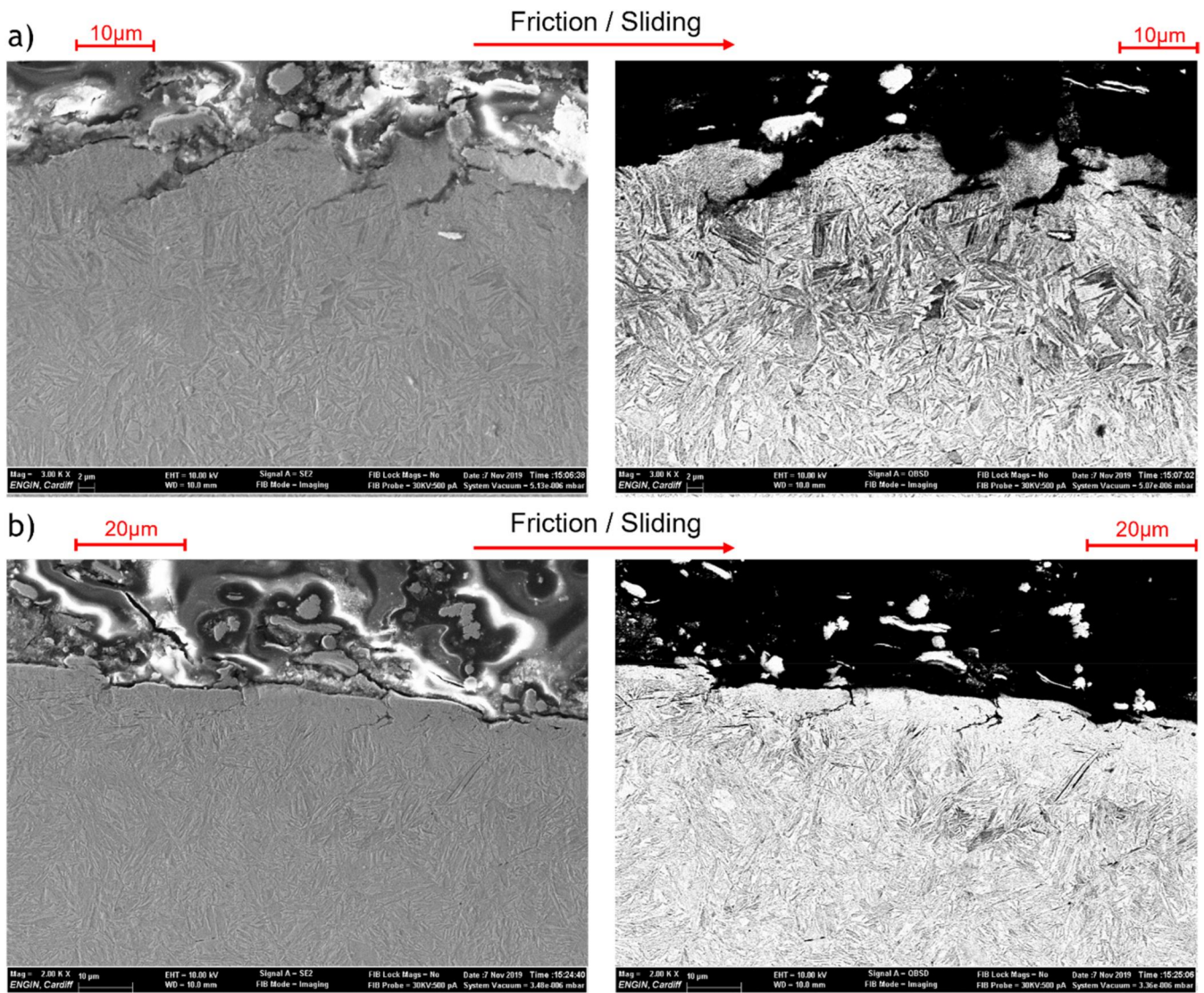
Figure 23. Secondary electron (left) and back-scattered electron images of cracks in the near surfaces of the pitted areas of a) fast and b) slow disk from Test 1.

micropitted after 1×10^5 cycles (fast surface), showed strong SRR effects and clear entrainment effects for both surfaces. N3, a parameter primarily controlled by early stage micropitting, was dominated by SRR on the fast surface and retained the entrainment effect for the slow surface despite a reduced SRR effect. Where effects were seen, SRR always increased the extent of micropitting, while entrainment protected the surface from fatigue.

SRR and entrainment effects continued to influence the fast surface throughout the duration of the test; however, this was not the case for the slow surface. Test stages in this work were based on the fast surface cycles, and the unequal numbers of slow disk cycles between tests of differing SRR certainly has an influence on the fatigue. It is unlikely that this can completely account for the difference in effects, however, as if this was the case the difference in cycles would cancel out the SRR effect exactly. This is unlikely, and even more so when it is recalled that the centerpoint test results for the slow surface typically indicated linear behavior, while a nonlinear indication would be expected if this were the case.

A previous work in the literature (7) found the SRR effect on micropitting fatigue was proportional to the total sliding distance. This work does not support this for a simple reason: in each test of a twin-disk rig, both fast and slow surfaces must slide the same distance relative to each other. However, the SRR effect calculated is different for the fast and slow surfaces.

One possibility considered was that the differences between micropitting effects on the fast and slow surfaces, particularly for SRR, may be due to differing mechanisms of crack propagation being present on each surface. Microscope investigations of disk sections, such as shown in Fig. 23, confirmed that the cracks on both surfaces propagated against the direction of friction, which was in line with common understanding.

In this case, crack pressurization and fluid entrapment mechanisms discussed in the literature (10) are likely to be far more significant on the slow surface, as on the fast surface the lubricant would be forced out of the crack by the approaching contact, as illustrated in Fig. 24. However, there remains much debate around these phenomena, and this
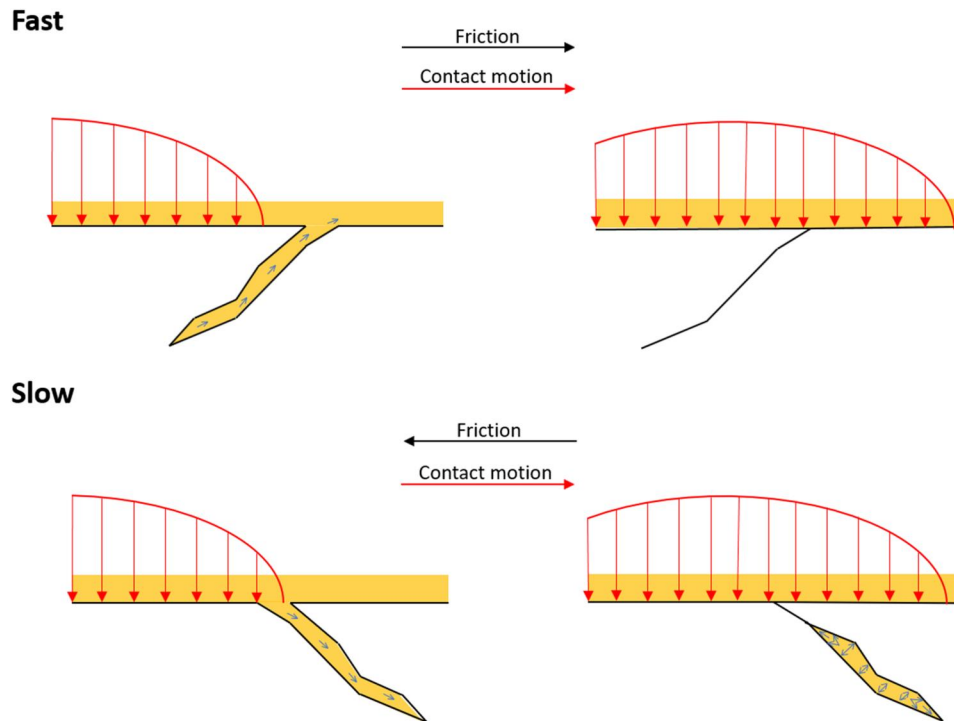
Fast

Slow

Figure 24. Differences in the behavior of lubricant in surface cracks on the fast and slow surfaces.

hypothesis cannot be confirmed without further investigation, hence the cause of the differences in SRR effects remains unresolved.

The entrainment effect is almost certainly due to the increase in lubricant film thickness with entrainment, more effectively protecting the surfaces from direct contact. The effect of entrainment on the slow surface decreased as the test went on. However, the strong initial effects suggest that film thickness influences the initiation of fatigue cracks or has an accelerating effect on micropit production in the early stages.

A key finding of this work is that the effects of pressure, SRR, and entrainment velocity are not restricted to acting simply as single factor effects and that their micropitting interactions go beyond even the two-factor effects seen in previous research. (11, 19) Three-factor effects were observed for all of the parameters considered, highlighting that micropitting fatigue is the result of an interconnected network of factors which determine the final contact conditions.

Due to the volume of experimental work involved (each test required approximately 1 month to complete, plus additional time for data analysis), it was not possible to conduct repeat tests within an acceptable timeframe. As such, further experimental and numerical work is required to assess the statistical significance of the results and potential applications.

The adoption of a factorial test design for this work enabled the analysis of two- and three- factor interaction effects that would not be possible through assessment of individual parameters alone. The complexity of analysis and restriction of the tests to only high and low settings (a factorial program with high, middle, and low settings for three

variables would allow analysis of nonlinear effects, but requires an impractical 27 tests as a minimum) do certainly present limitations to their use. However, factorial and fractional-factorial tests provide an incredibly valuable means of screening many variables efficiently and thus highlighting potential areas for future work at closer detail, and remain one of the only means of assessing interaction effects. As such, the authors believe these designs remain a valuable, albeit rarely used, tool for tribological research.

Conclusions

A full-factorial experimental program was conducted using a twin-disk test rig to investigate the effects of pressure, SRR, and entrainment velocity on early-stage micropitting. The conclusions of the work can be summarized as follows:

- Pressure showed the strongest influence of the three variables on the micropitted area, micropit depth, volume removed, and rate of micropitting later in the tests for both the fast and slow surfaces. Increased contact pressure acted to increase micropitting in all cases. The influence of pressure was greatest later in the tests, but weaker during the micropitting initiation phase.
- SRR was the strongest factor influencing micropitting initiation for both surfaces, with greater sliding leading to increased micropitting. SRR was a strong influence throughout the tests for the fast surface, but decreased markedly in strength for the slow surface as the tests progressed.
- Increased entrainment velocity opposed micropitting for both surfaces, but as with SRR the effect of entrainment

velocity on the slow surface decreased as the tests went on.

- Extensive two- and three-factor interaction effects were observed for both the fast and slow surfaces, showing micropitting to be influenced by a complex network of interconnected effects.

Disclosure statement

The authors report that there are no competing interests to declare.

Funding

References

(1) Keller, J., Gould, B., Greco, A. (2017), Investigating Bearing Failures in Wind Turbine Drivetrains. In Boulder, Colorado, USA [cited 2017 Dec 12]. Available from: http://windtechconferences.org/wp-content/uploads/2017/10/Keller-Jonathan-Abstract-for-Invited-Talk.pdf

(2) Kotzalas, M. N., and Doll, G. L. (2010), "Tribological advancements for reliable wind turbine performance," *Philosophical Transactions. Series A, Mathematical, Physical, and Engineering Sciences*, **368,** pp 4829–4850. doi:10.1098/rsta.2010.0194

(3) Ariura, Y. A., Ueno, T., and Nakanishi, T. (1983), "An Investigation of Surface Failure of Surface Hardened Gears by Scanning Electron Microscopy Observations," *Wear*, **87,** pp 305–316. doi:10.1016/0043-1648(83)90134-5

(4) Clarke, A., Evans, H., and Snidle, R. (2016), "Understanding micropitting in gears," *Proceedings of the Institution of Mechanical Engineers, Part C: Journal of Mechanical Engineering Science*, **230,** pp 1276–1289. doi:10.1177/0954406215606934

(5) Errichello, R. L. (2012), "Morphology of Micropitting," *Gear Technology*, **29**(8), pp 74–81.

(6) Olver, A. V. (2005), "The Mechanism of Rolling Contact Fatigue: An Update," *Proceedings of the Institution of Mechanical Engineers, Part J: Journal of Engineering Tribology*, **219**, pp 313–330. doi:10.1243/135065005X9808

(7) Kadiric, A., and Rycerz, P. (2016), "Influence of Contact Conditions on the Onset of Micropitting in Rolling-Sliding Contacts Pertinent to Gear Applications," *AGMA Technical Paper 16FTM21*, AGMA: Virginia, USA

(8) L'Hostis, B., Minfray, C., Frégonèse, M., Verdu, C., Ter-Ovanessian, B., Vacher, B., Le Mogne, T., Jarnias, F., and Da-Costa D'Ambros, A. (2017), "Influence of Lubricant Formulation on Rolling Contact Fatigue of Gears – Interaction of Lubricant Additives with Fatigue Cracks," *Wear*, **382-383**, pp 113–122. doi:10.1016/j.wear.2017.04.025

(9) Way, S. (1935), "Pitting due to Rolling Contact.pdf," *Journal of Applied Mechanics*, **2**, pp A-49–A-58.

(10) Bower, A. F. (1988), "The Influence of Crack Face Friction and Trapped Fluid on Surface Initiated Rolling Contact Fatigue Cracks," *Journal of Tribology*, **110**, pp 704–711. doi:10.1115/1.3261717

(11) Oila, A., and Bull, S. J. (2005), "Assessment of the Factors Influencing Micropitting in Rolling/Sliding Contacts," *Wear*, **258**, pp 1510–1524. doi:10.1016/j.wear.2004.10.012

(12) Oila, A., Shaw, B. A., Aylott, C. J., and Bull, S. J. (2005), "Martensite Decay in Micropitted Gears," *Proceedings of the Institution of Mechanical Engineers, Part J: Journal of Engineering Tribology*, **219**, pp 77–83. doi:10.1243/135065005X9790

(13) Warhadpande, A., Sadeghi, F., and Evans, R. D. (2013), "Microstructural Alterations in Bearing Steels under Rolling Contact Fatigue Part 1—Historical Overview," *Tribology Transactions*, **56**, pp 349–358. doi:10.1080/10402004.2012.754073

(14) Mallipeddi, D., Norell, M., Sosa, M., and Nyborg, L. (2017), "Influence of Running-In On Surface Characteristics Of Efficiency Tested Ground Gears," *Tribology International*, **115**, pp 45–58. doi:10.1016/j.triboint.2017.05.018

(15) D'Errico, F. (2011), "Micropitting Damage Mechanism on Hardened and Tempered, Nitrided, and Carburizing Steels," *Materials and Manufacturing Processes*, **26**, pp 7–13. doi:10.1080/10426910903388424

(16) Ahlroos, T., Ronkainen, H., Helle, A., Parikka, R., Virta, J., and Varjus, S. (2009), "Twin Disc Micropitting Tests," *Tribology International*, **42**, pp 1460–1466. doi:10.1016/j.triboint.2009.05.023

(17) Krantz, T. (2005), *The influence of roughness on gear surface fatigue*. U.S. Army Research Laboratory, Glenn Research Center: Cleveland, Ohio.

(18) Krantz, T. L., Alanou, M. P., Evans, H. P., and Snidle, R. W. (2001), "Surface Fatigue Lives of Case-Carburized Gears With an Improved Surface Finish," *Journal of Tribology*, **123**, pp 709–716. doi:10.1115/1.1387036

(19) Li, S., and Kahraman, A. (2013), "Micro-Pitting Fatigue Lives Of Lubricated Point Contacts: Experiments and Model Validation," *International Journal of Fatigue*, **48,** pp 9–18. doi:10.1016/j.ijfatigue.2012.12.003

(20) Benjayati, C., Olver, A. V., and Hamer, C. J. (2003), "An Experimental Study of Micropitting Using a New Miniature Test rig.pdf," In *Transient Processes in Tribology*. Elsevier: Lyon, France. (Tribology Series, 43).

(21) Lainé, E., Olver, A. V., and Beveridge, T. A. (2008), "Effect of Lubricants on Micropitting and Wear," *Tribology International*, **41**, pp 1049–1055. doi:10.1016/j.triboint.2008.03.016

(22) Brizmer, V., Pasaribu, H. R., and Morales-Espejel, G. E. (2013), "Micropitting Performance of Oil Additives in Lubricated Rolling Contacts," *Tribology Transactions*, **56**, pp 739–748. doi:10.1080/10402004.2013.790097

(23) Morales-Espejel, G. E., Rycerz, P., and Kadiric, A. (2018), "Prediction of Micropitting Damage in Gear Teeth Contacts Considering the Concurrent Effects of Surface Fatigue and Mild Wear," *Wear*, **398-399**, pp 99–115. doi:10.1016/j.wear.2017.11.016

(24) Zhou, Y., Zhu, C., and Liu, H. (2019), "A Micropitting Study Considering Rough Sliding and Mild Wear," *Coatings*, **9**, pp 639. doi:10.3390/coatings9100639

(25) Liu, H., Liu, H., Zhu, C., and Tang, J. (2020), "Study on Gear Contact Fatigue Failure Competition Mechanism Considering Tooth Wear Evolution," *Tribology International*, **147**, pp 106277. doi:10.1016/j.triboint.2020.106277

(26) Moorthy, V., and Shaw, B. A. (2012), "Contact Fatigue Performance of Helical Gears with Surface Coatings," *Wear*, **276-277,** pp 130–140. doi:10.1016/j.wear.2011.12.011

(27) Moorthy, V., and Shaw, B. A. (2013), "An Observation on the Initiation of Micro-Pitting Damage in As-Ground and Coated Gears during Contact Fatigue," *Wear*, **297,** pp 878–884. doi:10.1016/j.wear.2012.11.001

(28) Zhang, J., and Shaw, B. (2016), "Performance of Gears with WC/C Coating," *Power Transmissions: Proceedings of the International Conference on Power Transmissions 2016 (ICPT 2016), Chongqing, PR China*, 27-30 October 2016, pp 357–360, Taylor & Francis: Chongqing, P.R. China.

(29) Singh, H., Ramirez, G., Eryilmaz, O., Greco, A., Doll, G., and Erdemir, A. (2016), "Fatigue Resistant Carbon Coatings for Rolling/Sliding Contacts," *Tribology International*, **98**, pp 172–178. doi:10.1016/j.triboint.2016.02.008

(30) Zhou, Y., Zhu, C., Gould, B., Demas, N. G., Liu, H., and Greco, A. C. (2019), "The Effect of Contact Severity on Micropitting: Simulation and Experiments," *Tribology International*, **138**, pp 463–472. doi:10.1016/j.triboint.2019.06.020

(31) Rabaso, P., Gauthier, T., Diaby, M., and Ville, F. (2013), "Rolling Contact Fatigue: Experimental Study of the Influence of Sliding, Load, and Material Properties on the Resistance to Micropitting of Steel Discs," *Tribology Transactions*, **56**, pp 203–214. doi:10.1080/10402004.2012.737504

(32) Morales-Espejel, G. E., and Brizmer, V. (2011), "Micropitting Modelling in Rolling–Sliding Contacts: Application to Rolling Bearings," *Tribology Transactions*, **54**, pp 625–643. doi:10.1080/10402004.2011.587633

(33) Cen, H., Morina, A., and Neville, A. (2018), "Effect of Slide to Roll Ratio on the Micropitting Behaviour in Rolling-Sliding Contacts Lubricated with ZDDP-Containing Lubricants," *Tribology International*, **122**, pp 210–217. doi:10.1016/j.triboint.2018.02.038

(34) Tallian, T. E. (1967), "On Competing Failure Modes in Rolling Contact," *A S L E Transactions*, **10**, pp 418–439. doi:10.1080/05698196708972201

(35) Krantz, T. L. (2015), "On the Correlation of Specific Film Thickness and Gear Pitting Life," *Gear Technology*, **32**(1), pp 52–62.

(36) Sharif, K. J., Evans, H. P., and Snidle, R. W. (2012), "Modelling of Elastohydrodynamic Lubrication and Fatigue of Rough Surfaces: The Effect of Lambda Ratio," *Proc IMechE Part J: J Engineering Tribology*, **226**, pp 1039–1050. doi:10.1177/1350650112458220

(37) NIST/SEMATECH, NIST-SEMATECH e-Handbook of Statistical Methods, NIST, 2013, https://www.itl.nist.gov/div898/handbook/index.htm (accessed January 6, 2021).

(38) Crump, M. J. C., Navarro, D., and Suzuki, J. (2019), "Answering Questions with Data: Introductory Statistics for Psychology Students," doi:10.17605/OSF.IO/JZE52 (accessed January 6, 2021).

(39) Britton, W. M., Clarke, A., and Evans, H. P. (2021), "A Novel Method for Automatic Detection of Incipient Micropitting in Ground Surfaces," *Tribology International*, **159**, pp 106959. doi:10.1016/j.triboint.2021.106959